Protein Science (1993), *2*, 1331–1341. Cambridge University Press. Printed in the USA.

Backbone assignments and secondary structure of the *Escherichia coli* enzyme-II mannitol A domain determined by heteronuclear three-dimensional NMR spectroscopy

GERARD J.A. KROON,[1] JOACHIM GRÖTZINGER,[2] KLAAS DIJKSTRA,[1]
RUUD M. SCHEEK,[1] AND GEORGE T. ROBILLARD[1]

[1] The Bioson Institute, University of Groningen, Nijenborgh 4, 9747 AG Groningen, The Netherlands
[2] Institut für Biochemie, Rheinisch-Westfälische Technische Hochschule Aachen, Klinikum, Pauwelsstrasse 16, D-5100 Aachen, Germany

(RECEIVED April 20, 1993; REVISED MANUSCRIPT RECEIVED June 14, 1993)

Abstract

This report presents the backbone assignments and the secondary structure determination of the A domain of the *Escherichia coli* mannitol transport protein, enzyme-II^{mtl}.

The backbone resonances were partially assigned using three-dimensional heteronuclear ^{1}H NOE ^{1}H-^{15}N single-quantum coherence (^{15}N NOESY-HSQC) spectroscopy and three-dimensional heteronuclear ^{1}H total correlation ^{1}H-^{15}N single-quantum coherence (^{15}N TOCSY-HSQC) spectroscopy on uniformly ^{15}N enriched protein. Triple-resonance experiments on uniformly ^{15}N/^{13}C enriched protein were necessary to complete the backbone assignments, due to overlapping ^{1}H and ^{15}N frequencies. Data obtained from three-dimensional ^{1}H-^{15}N-^{13}Cα correlation experiments (HNCA and HN(CO)CA), a three-dimensional ^{1}H-^{15}N-^{13}CO correlation experiment (HNCO), and a three-dimensional ^{1}Hα-^{13}Cα-^{13}CO correlation experiment (COCAH) were combined using SNARF software, and yielded the assignments of virtually all observed backbone resonances.

Determination of the secondary structure of IIA^{mtl} is based upon NOE information from the ^{15}N NOESY-HSQC and the ^{1}Hα and ^{13}Cα secondary chemical shifts. The resulting secondary structure is considerably different from that reported for IIA^{glc} of *E. coli* and *Bacillus subtilis* determined by NMR and X-ray.

Keywords: mannitol; NMR; phosphoenolpyruvate-dependent phosphotransferase system; protein structure determination; triple resonance

Reprint requests to: Ruud M. Scheek, The Bioson Institute, University of Groningen, Nijenborgh 4, 9747 AG Groningen, The Netherlands.

Abbreviations: 2D, 3D NMR, two-dimensional, three-dimensional nuclear magnetic resonance; NOE, nuclear Overhauser effect; ^{15}N NOESY-HSQC, 3D ^{1}H NOE ^{1}H-^{15}N heteronuclear single-quantum coherence spectroscopy; ^{15}N TOCSY-HSQC, 3D ^{1}H total correlation ^{1}H-^{15}N heteronuclear single-quantum coherence spectroscopy; HNCA, HN(CO)CA, 3D ^{1}H-^{15}N-^{13}Cα correlation spectroscopy; HNCO, 3D ^{1}H-^{15}N-^{13}CO correlation spectroscopy; COCAH, 3D ^{13}CO-^{13}Cα-^{1}Hα correlation spectroscopy; FTIR, Fourier transform infrared; SDS-PAGE, sodium dodecyl sulfate–polyacrylamide gel electrophoresis; TPPI, time proportional phase incrementation; rf, radio frequency; PTS, phosphoenol-pyruvate dependent phosphotransferase system; fru, fructose; glc, glucose; mtl, mannitol; PEP, phosphoenol-pyruvate; HPr, histidine-containing protein; EI, enzyme-I; EII, enzyme-II; EII^{mtl}, enzyme-II mannitol; TSP, trimethylsilylpropionic acid; TMS, trimethylsilyl-propanesulfonic acid; IPTG, iso-propyl-β-D-thiogalactoside; IIA^{mtl}, the A domain of enzyme-II mannitol; IIA^{glc}, the A domain of enzyme-II glucose; IIB^{mtl}, the B domain of enzyme-II mannitol.

The enzyme-II mannitol of *Escherichia coli* is part of the phosphoenol-pyruvate dependent phosphotransferase system. The system regulates the uptake and phosphorylation of specific carbohydrate substrates (for reviews see Postma & Lengeler [1985], Meadow et al. [1990], and Lolkema & Robillard [1992]). Before the substrate is phosphorylated, a phosphoryl group is transferred from PEP via enzyme-I and the histidine containing protein to EII^{mtl}.

EII^{mtl} is a 67-kDa membrane bound protein consisting of three domains—A, B, and C—linked via flexible parts. The cytoplasmic carboxy-terminal A domain transfers the phosphoryl group from HPr to the cytoplasmic B domain, which phosphorylates the mannitol after translocation through the membrane by the N-terminal C domain.

IIA^{mtl} is phosphorylated at the Nϵ2 position of His 554 (Van Dijk et al., 1992) by phospho-HPr and transfers the

phosphoryl group to the Cys 384 of IIB^{mtl} (Pas & Robillard, 1988; Pas et al., 1988, 1991). Substitution of an alanine for His 554 inhibits the PEP-dependent mannitol phosphorylation reaction.

Van Weeghel et al. (1991) have cloned the cytoplasmic A domain and brought it to overexpression in *E. coli*. The phosphorylation site histidine of the 16.4-kDa cloned A domain is now located at position 65 and is still functional. Achieving a separate subcloned and functional domain not only allows us to study structural features of the domain, but it also enables us to study the interactions between IIA^{mtl} and HPr (Haris et al., 1992; Van Dijk, 1992; Van Nuland et al., 1993).

Multidimensional heteronuclear NMR spectroscopy has been used to identify secondary structure elements of the IIA^{glc} from *E. coli* (Pelton et al., 1991) and *Bacillus subtilis* (Fairbrother et al., 1991). Neither protein has sequential homology with IIA^{mtl}, although they have similar functions in the PTS. Both proteins contain a considerable amount of β-sheet, but only small helical elements have been observed. In contrast to these proteins, a large amount of α-helix and a relatively small amount of β-sheet has been observed for IIA^{mtl} using CD (Van Nuland, pers. comm.) and FTIR measurements (Haris et al., 1992). This paper reports the backbone assignments and secondary structure determination of IIA^{mtl}, the first step toward the determination of the 3D structure in solution, and compares the secondary structure of IIA^{mtl} with that of IIA^{glc} of *E. coli* and *B. subtilis*.

Results

The HSQC experiment

The 2D ^1H-^{15}N HSQC spectrum (Bodenhausen & Ruben, 1980) recorded at 30 °C (Fig. 1) shows many overlapping ^1H-^{15}N frequency pairs, especially at ω^1H 9.3 ppm and $\omega^{15}N$ 127 ppm (F13 and F81), at ω^1H 8.7–8.8 ppm and $\omega^{15}N$ 131 ppm (V137, A105, L57, and F90), and in the region between ω^1H 7.2–9.0 ppm and $\omega^{15}N$ 115–123 ppm. The overlap in this latter region is shown in more detail in Figure 1B.

Of the expected 144 ^1H-^{15}N backbone frequency pairs, only 125 pairs were found in the spectrum recorded at 30 °C. This was caused not only by spectral overlap but also by too rapid exchange of some amide protons with water at the pH used. The protein is unstable at pH values below 7.0, where exchange would be slower.

Backbone assignment

The first step in the backbone assignment procedure was to find sequential connectivities using a method described by Van Nuland et al. (1992), combining information from the NOESY-HSQC and TOCSY-HSQC spectra (Billeter et al., 1982; Wüthrich, 1986).

Preliminary backbone assignments were found by searching for small residues like glycines and alanines within stretches of sequential connectivities, because these residues could be identified most reliably in the TOCSY-HSQC spectra. Most other types of residues showed only the ^1HN and $^1H\alpha$ frequencies in the TOCSY spectra. This procedure enabled us to assign 40% of the backbone amide and ^{15}N resonances. Constant time triple-resonance experiments were necessary in order to confirm and extend the assignments.

In the HN(CO)CA experiment, the ^1H-$^{15}N(i)$ pair is labeled with the $^{13}C\alpha(i-1)$ frequency. In the HNCA experiment, the same pair is labeled with both the $^{13}C\alpha(i)$ and the $^{13}C\alpha(i-1)$ frequencies. A sequential connectivity is found by picking the $^{13}C\alpha(i-1)$ frequency corresponding to the ^1H-$^{15}N(i)$ pair in the HN(CO)CA and searching for a ^1H-$^{15}N(i-1)$ pair in the HNCA with a matching $^{13}C\alpha$ frequency (Fig. 2, step 1).

Stretches of sequentially assigned resonances were placed in the amino acid sequence using the fact that four prolines are present in the protein resulting in five stretches, each with a specific number of residues. All 11 glycines were identified by their characteristic $^{13}C\alpha$ chemical shift (Van Nuland et al., 1992), which ranges from 43.0 to 48.5 ppm, whereas the $^{13}C\alpha$ chemical shifts of all other residues range from 49.7 to 66.9 ppm (see Table 1). Using these features, about 80% of the backbone resonances could be assigned. The remaining ^1H-^{15}N pairs could not be connected unambiguously due to overlapping $^{13}C\alpha$ frequencies.

To resolve these ambiguities, the HNCO and COCAH spectra were used. In combination with the TOCSY-HSQC, these spectra provide an independent way to find connectivities. In the HNCO experiment the ^1H-$^{15}N(i)$ pair is labeled with the $^{13}CO(i-1)$ frequency. In the COCAH experiment the $^1H\alpha(i)$ resonance is labeled with the $^{13}CO(i)$ and $^{13}C\alpha(i)$ frequencies. To check whether the ^1H-^{15}N-$^{13}C\alpha$ triple found in step 1 (Fig. 2) can be assigned to residue $(i-1)$, we used the $H\alpha$ resonance of that residue, identified in the TOCSY-HSQC (Fig. 2, step 2), in combination with the $^{13}C\alpha$ frequency, to find the ^{13}CO frequency of that residue in the COCAH spectrum (Fig. 2, step 3). When this ^{13}CO frequency matches with the one found in the HNCO spectrum at the ^1H-$^{15}N(i)$ frequency (Fig. 2, step 4), the connectivity is accepted. This procedure is illustrated for residues A62 and V63 in Figure 3.

The connectivities were confirmed by comparing both ^1H-^1H NOESY slices from the NOESY-HSQC for sequential NOEs. Using this procedure we were able to check all previously obtained sequential connectivities and to find most of the remaining connectivities (Van Nuland et al., 1992).

All backbone assignments obtained thus far are presented in Table 1. Figure 4 shows the $^1H\alpha$-$^{13}C\alpha$ ($\omega1$-$\omega2$) and $^1H\alpha$-^{13}CO ($\omega1$-$\omega3$) projections of the COCAH ex-

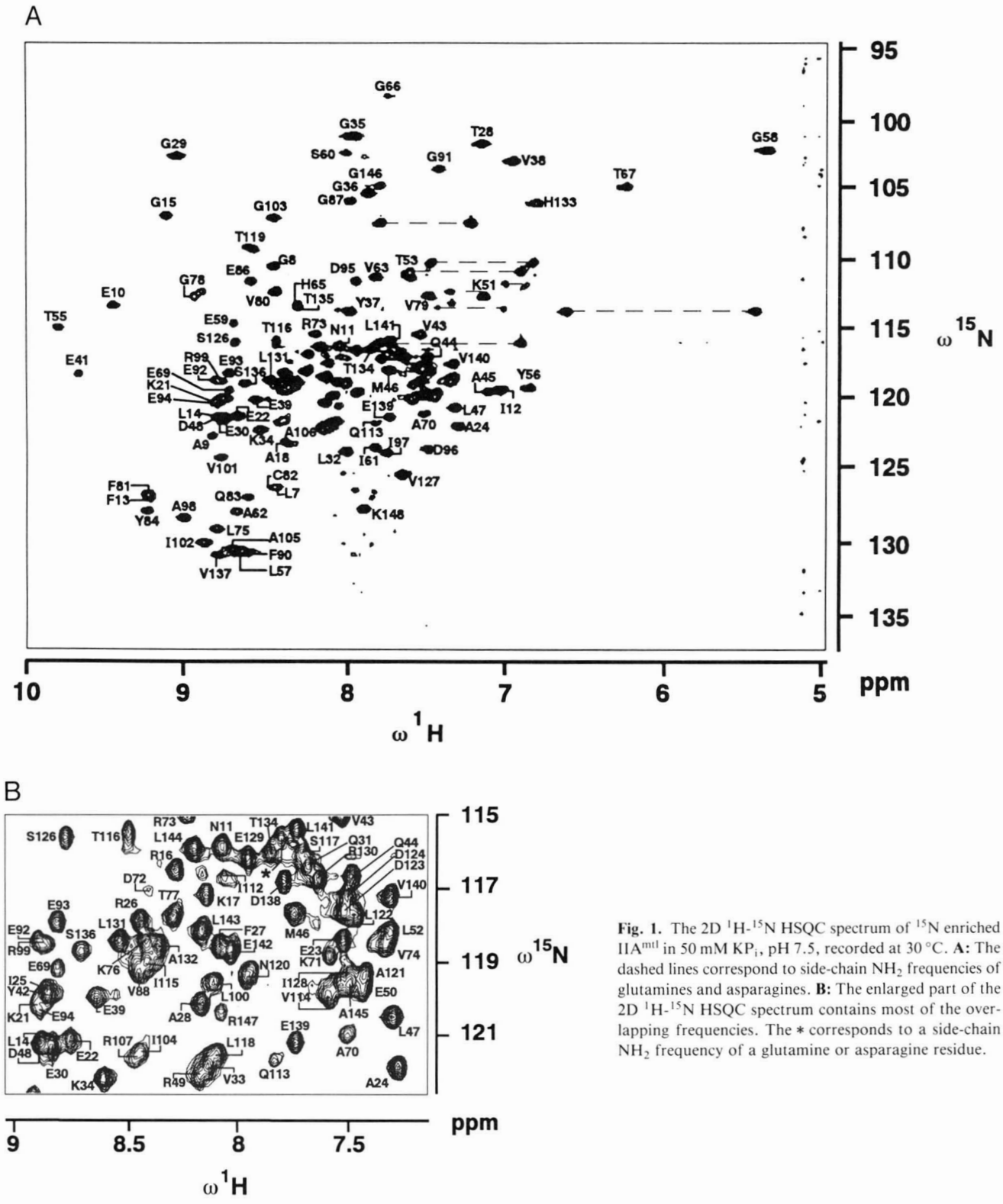

Fig. 1. The 2D ^{1}H-^{15}N HSQC spectrum of ^{15}N enriched IIA^{mtl} in 50 mM KP_i, pH 7.5, recorded at 30 °C. **A:** The dashed lines correspond to side-chain NH_2 frequencies of glutamines and asparagines. **B:** The enlarged part of the 2D ^{1}H-^{15}N HSQC spectrum contains most of the overlapping frequencies. The * corresponds to a side-chain NH_2 frequency of a glutamine or asparagine residue.

periment, with many of the assignments indicated. Due to the relatively narrow ^{13}CO resonances, the resolution in the ^{13}CO domain is comparable to that in the $^{13}C\alpha$ domain, although the spectral width in the ^{13}CO domain is half that in the $^{13}C\alpha$ domain.

Determination of the secondary structure elements

The NOESY-HSQC recorded at 30 °C was analyzed for patterns in amide–amide (NN) and Hα–amide (αN) NOEs that are characteristic of specific secondary struc-

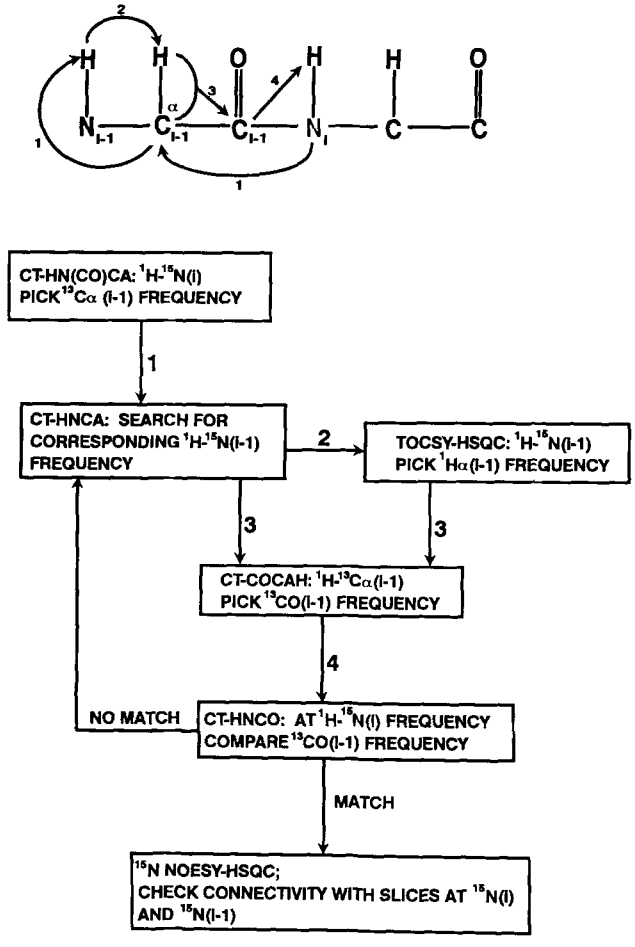

Fig. 2. Schematic representation of the strategy used to find the backbone connectivities. See text for explanation.

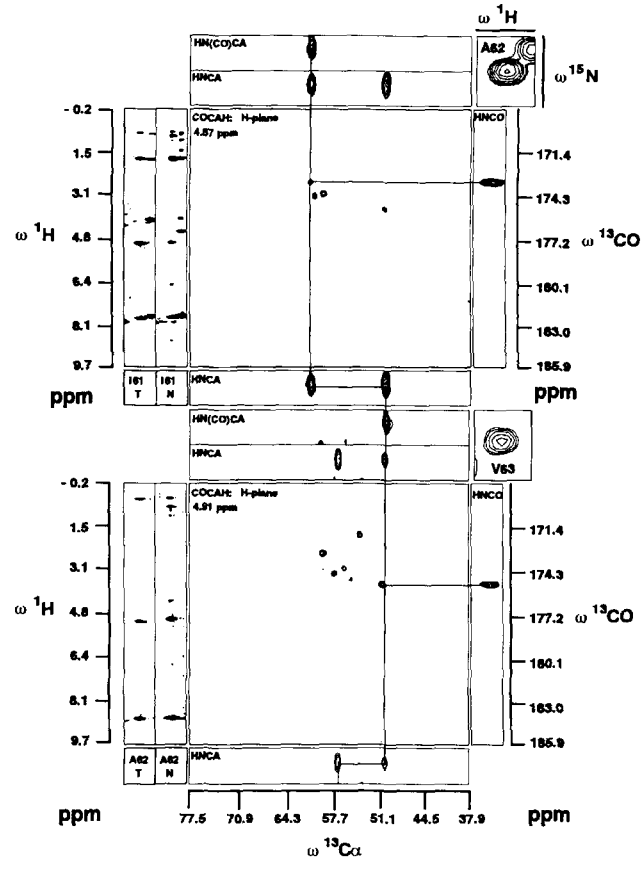

Fig. 3. Example of two sequential connectivities found using the scheme of Figure 2. The peak in the upper right view is part of the ^{1}H-^{15}N projection of the HNCA spectrum. The three ^{13}C slices are taken from the HN(CO)CA, HNCA, and HNCO spectra at the same ^{15}N and ^{1}H frequencies. When a connectivity has been found, the ^{1}H-^{1}H slices from the TOCSY-HSQC (T) and NOESY-HSQC (N) of the previous residue are shown together with the ^{13}Cα-^{13}CO plane taken from the COCAH spectrum at the ^{1}Hα frequency of the previous residue. The lines connecting the peaks represent the sequential walk.

ture elements (Fig. 5A) (Wüthrich, 1986). Additional evidence comes from an analysis of the chemical shifts (Fig. 5B). The $\alpha N(i, i+1)$ NOEs were classified as strong, medium, or weak. A region was classified as a helix when $NN(i, i+1)$ NOEs were observed in combination with $\alpha N(i, i+3)$ NOEs, weak $\alpha N(i, i+1)$ NOEs, positive $^{13}C\alpha$ (Spera & Bax, 1991), and negative $^1H\alpha$ secondary chemical shifts (Wishart et al., 1992). A region was classified as a β-strand if $\alpha N(i, i+3)$ NOEs were absent, $\alpha N(i, i+1)$ NOEs were strong, and there were negative $^{13}C\alpha$ and positive $^1H\alpha$ secondary chemical shifts. Also shown in Figure 5B are the ^{13}CO secondary chemical shifts, which display a dependency on secondary structure similar to, albeit less pronounced than, the $^{13}C\alpha$ secondary shifts.

This analysis yielded evidence for five helical regions—E22–K34, E41–K51, I111–A121, S126–T134, and D138–L142—and two β-strands—T77–Y84 and R99–A105 (Fig. 5A). Based on chemical shift evidence (Fig. 5B), two extra regions (residues N11–A18 and T55–H65) would appear to be β-strands, but the NOE evidence (Fig. 5A) does not warrant this conclusion. In addition, several of the NOEs connecting the two β-strands could be identified. As indicated in Figure 6, these two strands combine to form an anti-parallel β-sheet in IIA^{mtl}.

Discussion

It was impossible to obtain complete backbone assignments of *E. coli* IIA^{mtl} domain using only ^{15}N-^{1}H heteronuclear NMR experiments. The ^{15}N NOESY-HSQC and TOCSY-HSQC spectra yielded about 40% of the amide proton resonance assignments. This was caused by spectral overlap and incomplete TOCSY-HSQC spectra. After analyzing the HNCA and HN(CO)CA spectra, in combination with the previous ones, 80% of the amide proton resonances present could be assigned. When the HNCO and COCAH spectra were included, almost all

Table 1. *Backbone ^{1}H, ^{15}N, and ^{13}C chemical shifts for the IIA^{mtl} domain of E. coli in 50 mM KP_i, pH 7.3–7.5, at 30 °C*[a]

Residue	HN	^{15}N	Hα	$^{13}C\alpha$	^{13}CO	Residue	HN	^{15}N	Hα	$^{13}C\alpha$	^{13}CO
1 Met						75 Leu	8.85	129.3	4.27	55.6	177.6
2 Ala						76 Lys	8.39	118.3	4.42	54.9	172.6
3 Asn						77 Thr	8.25	117.6	4.62	62.3	175.0
4 Leu						78 Gly	8.98	112.2	3.76/2.97	44.8	169.3
5 Phe						79 Val	7.44	112.2	5.04	58.3	174.2
6 Lys						80 Val	8.47	112.1	5.08	58.4	173.2
7 Leu[b]	8.43	126.3		54.3	174.9	81 Phe	9.31	126.8	4.75	56.8	172.7
8 Gly	8.48	110.1	4.48/3.85	43.0	173.7	82 Cys	8.48	126.2	5.43	55.6	171.0
9 Ala	8.88	122.6	3.78	55.0	179.1	83 Gln	8.66	127.0	4.64	54.0	172.4
10 Glu	9.55	113.0	4.20	57.2	176.2	84 Tyr	9.30	128.1	5.16	54.1	174.9
11 Asn	8.05	115.9	5.12	53.1	172.0	85 Pro			4.17	65.3	178.4
12 Ile	7.02	119.1	4.74	59.8	173.5	86 Glu	8.63	111.3	4.31	56.3	177.7
13 Phe	9.28	127.0	4.74	56.6	174.0	87 Gly	7.98	105.3	4.07/3.96	43.6	172.4
14 Leu	8.85	121.2	4.69	53.4	179.0	88 Val	8.42	119.2	4.22	59.8	174.8
15 Gly	9.16	106.4	3.85/3.47	46.9	174.6	89 Arg	9.14	131.8	3.85	58.1	175.1
16 Arg	8.25	116.6	4.06	53.1	174.3	90 Phe	8.67	130.9	4.66	57.0	175.6
17 Lys	8.12	117.3	4.66	55.3	175.2	91 Gly	7.41	103.0	4.63/3.97	43.5	173.1
18 Ala	8.41	123.0	4.59	51.5	174.9	92 Glu	8.86	118.4	4.12	57.8	178.0
19 Ala	8.74[c]	121.5[c]	4.40	52.6	177.8	93 Glu	8.77	118.0	4.54	54.4	178.2
20 Thr	7.14	101.2	4.72	57.7	174.8	94 Glu	8.85	120.3	3.73	58.8	176.3
21 Lys	8.87	120.1	3.50	57.8	176.9	95 Asp	7.95	111.2	4.70	52.9	176.7
22 Glu	8.71	121.0	3.61	60.9	178.1	96 Asp	7.48	123.4	4.55	52.6	174.6
23 Glu	7.52	118.4	3.97	58.7	179.1	97 Ile	7.75	123.7	4.05	58.8	174.6
24 Ala	7.28	121.7	4.44	54.3	179.5	98 Ala	9.05	128.4	4.53	50.2	175.8
25 Ile	8.81	119.7	3.45	66.2	177.0	99 Arg	8.84	118.6	5.13	55.3	174.2
26 Arg	8.42	117.9	3.82	59.9	177.7	100 Leu	8.10	119.6	4.71	53.0	173.6
27 Phe	8.07	118.6	4.19	61.8	176.9	101 Val	8.82	124.1	4.31	60.6	173.6
28 Ala	8.14	120.0	3.66	54.5	179.3	102 Ile	8.93	130.3	5.17	58.4	175.5
29 Gly	9.10	102.1	3.82/3.67	48.5	174.6	103 Gly	8.49	106.7	2.89/2.89	44.4	172.9
30 Glu	8.80	121.3	3.88	59.0	179.5	104 Ile	8.41	121.4	4.61	59.7	174.7
31 Gln	7.67	116.5	4.13	56.3	180.0	105 Ala	8.75	130.7	4.52	50.6	172.8
32 Leu	8.01	123.6	4.31	57.4	179.0	106 Ala	8.36	123.1	4.53	50.3	175.9
33 Val	8.11	121.7	4.03	64.7	180.9	107 Arg	8.44	121.7	4.19	55.6	178.0
34 Lys	8.57	122.0	4.03	58.9	178.4	108 Asn					
35 Gly	7.96	100.6	4.27/3.70	44.5	173.0	109 Asn					
36 Gly	7.87	104.7	3.87/3.76	44.4	173.6	110 Glu					
37 Tyr	7.99	113.5	4.38	59.8	176.2	111 His					
38 Val	6.93	102.3	5.12	56.7	174.5	112 Ile	8.04	116.9	3.71	62.8	177.9
39 Glu[c]	8.60	120.0			54.2	113 Gln	7.82	121.7	4.03	58.8	178.7
40 Pro			4.28	65.6	178.8	114 Val	7.57	119.9	3.63	65.9	177.4
41 Glu	9.75	118.0	4.20	59.4	177.7	115 Ile	8.38	119.1	3.44	65.6	178.1
42 Tyr	8.82	119.9	3.96	60.7	176.0	116 Thr	8.45	115.4	3.96	65.9	175.6
43 Val	7.53	115.2	3.49	66.9	177.6	117 Ser	7.70	115.9	4.29	61.5	176.9
44 Gln	7.48	116.9	3.83	57.2	177.1	118 Leu	8.06	121.5	4.12	57.3	178.2
45 Ala	7.10	119.3	4.25	54.1	179.5	119 Thr	8.64	108.9	3.83	65.2	177.2
46 Met	7.74	117.7	4.20	57.6	179.0	120 Asn	7.94	119.3	4.53	54.9	176.2
47 Leu	7.30	120.4	4.00	57.3	179.8	121 Ala	7.42	119.3	4.40	52.8	177.8
48 Asp	8.85	121.2	4.26	56.6	179.2	122 Leu	7.47	117.9	4.42	52.6	175.2
49 Arg	8.16	122.0	4.12	57.8	178.4	123 Asp	7.51	117.6	4.54	53.8	175.4
50 Glu	7.44	119.9	3.91	56.9	177.0	124 Asp	7.53	117.2	4.42	52.6	175.2
51 Lys	7.12	112.3	3.97	57.1	177.5	125 Glu	9.11[c]	126.5[c]	4.48	59.1	177.7
52 Leu	7.30	118.0	4.31	56.6	177.7	126 Ser	8.74	115.7	4.38	60.8	177.1
53 Thr	7.58	110.8	4.72	58.1	170.5	127 Val	7.66	125.4	3.72	65.9	177.2
54 Pro			4.88	62.5	179.1	128 Ile	7.53	119.4	3.72	65.7	177.0
55 Thr	9.87	114.5	4.40	62.0	175.2	129 Glu	7.96	116.4	4.09	58.9	179.2
56 Tyr	6.81	119.0	4.51	57.5	175.1	130 Arg	7.65	116.9	4.13	58.4	179.6
57 Leu	8.72	130.9	4.28	54.4	176.9	131 Leu	8.53	118.6	3.97	56.8	177.6
58 Gly	5.27	101.7	4.34/3.36	43.2	172.7	132 Ala	8.36	118.4	3.88	53.4	175.3
59 Glu	8.75	114.3	4.00	56.6	175.3	133 His	6.83	105.4	4.81	54.9	176.1
60 Ser	8.01	101.8	5.00	59.6	174.4	134 Thr	7.86	116.1	4.44	62.0	173.4
61 Ile	7.84	123.4	4.98	60.2	173.5	135 Thr	8.33	112.9	4.56	60.4	174.2
62 Ala	8.72	128.1	5.07	49.7	175.3	136 Ser	8.67	118.7	4.88	54.7	174.5
63 Val	7.82	110.9	5.68	56.3	171.1	137 Val	8.83	131.2	3.45	66.1	176.8
64 Pro			4.89	63.6	174.6	138 Asp	7.78	116.9	4.27	56.9	178.0
65 His	8.35	112.9	4.87	55.0	172.1	139 Glu	7.73	121.1	4.02	58.6	177.8
66 Gly	7.75	97.8	3.64/3.03	43.9	172.8	140 Val	7.32	117.3	3.28	66.0	177.1
67 Thr	6.18	104.3	4.38	59.9	176.4	141 Leu	7.73	115.6	3.74	57.2	179.6
68 Val	8.97[c]	122.0[c]	4.00	64.9	178.5	142 Glu	8.01	118.6	3.97	58.7	178.9
69 Glu	8.80	119.1	4.18	58.6	176.9	143 Leu	8.15	118.3	4.19	56.8	179.6
70 Ala	7.51	121.0	4.57	51.5	177.9	144 Leu	8.17	116.0	4.23	55.3	176.9
71 Lys	7.57	118.8	4.39	59.0	177.8	145 Ala	7.48	119.6	4.39	52.2	178.1
72 Asp	8.38	117.2	4.64	55.2	176.3	146 Gly	7.78	104.2	4.01/4.01	45.0	173.8
73 Arg	8.21	115.1	4.54	53.9	175.0	147 Arg	8.06	120.3	4.39	55.4	179.6
74 Val	7.33	118.4	3.90	62.8	174.4	148 Lys	7.90	127.8	4.19	56.9	181.1

[a] The ^{1}H chemical shifts are relative to TMS, the ^{15}N chemical shifts are relative to liquid NH_3 (Live et al., 1984), and the $^{13}C\alpha$ and ^{13}CO chemical shifts are relative to hypothetical internal TSP (Bax & Subramanian, 1986).

[b] No $^{1}H\alpha$ present in ^{15}N TOCSY-HSQC spectrum.

[c] Chemical shift obtained from ^{15}N HSQC recorded at 20 °C.

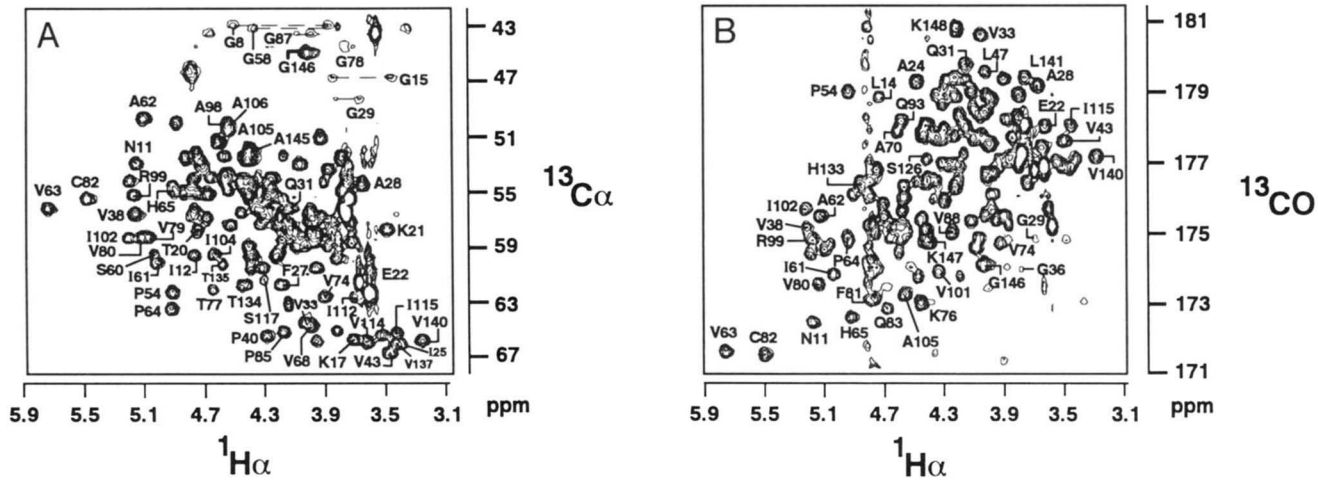

Fig. 4. The $^{1}H\alpha$-$^{13}C\alpha$ (**A**) and $^{1}H\alpha$-^{13}CO (**B**) projections of the COCAH spectrum of $^{15}N/^{13}C$ enriched IIA^{mtl} in 50 mM KP_i in $^{2}H_2O$ recorded at 30 °C. The dashed lines in the $^{1}H\alpha$-$^{13}C\alpha$ projection correspond to the glycine $^{1}H\alpha$ resonances. The intense peaks in both projections probably belong to the six N-terminal residues.

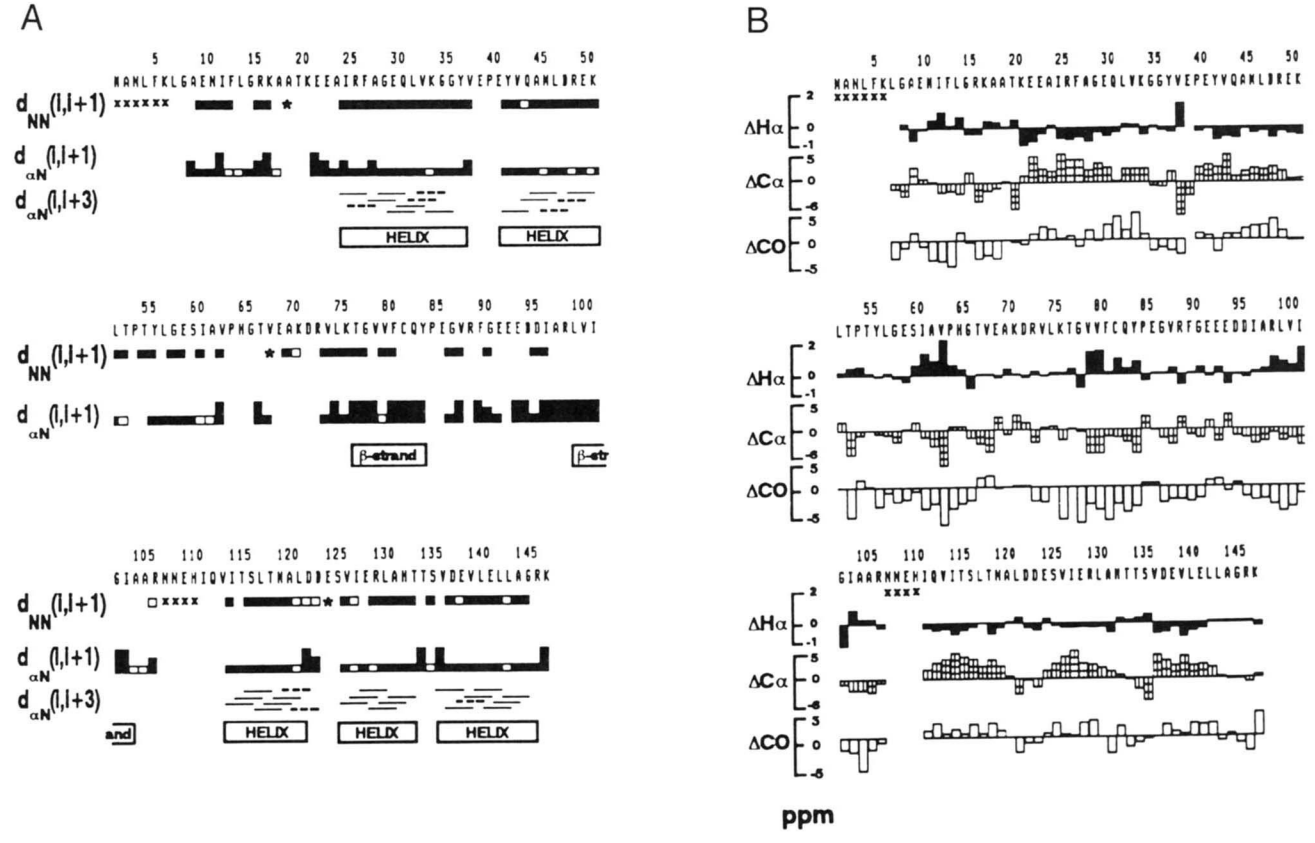

Fig. 5. A: Summary of the sequential NOEs involving the ^{1}HN protons, the $^{1}H\alpha$ protons, and the secondary structure elements as derived from the data. The $d_{\alpha N}(i, i+1)$ connectivities correspond to strong, medium, and weak NOEs, represented by large, medium, and small bars, respectively. The open bars in the $d_{\alpha N}(i, i+1)$ and $d_{NN}(i, i+1)$ connectivities and the dashed lines in the $d_{\alpha N}(i, i+3)$ connectivities represent ambiguities due to spectral overlap. **B:** Summary of the secondary chemical shifts of the $^{13}C\alpha$ ($\Delta C\alpha$), $^{1}H\alpha$ ($\Delta H\alpha$), and ^{13}CO (ΔCO) nuclei. The ^{13}CO secondary chemical shifts are calculated using random coil values relative to TMS (Howarth & Lilley, 1978). The $^{1}H\alpha$ secondary chemical shifts of the glycines are calculated by subtracting the average chemical shift of the two $H\alpha$'s from the random coil value (Wishart et al., 1992). Residues that are not observed in any of the spectra involving the amide protons are marked with X. Residues marked with * are only observed in the spectra recorded at 20 °C.

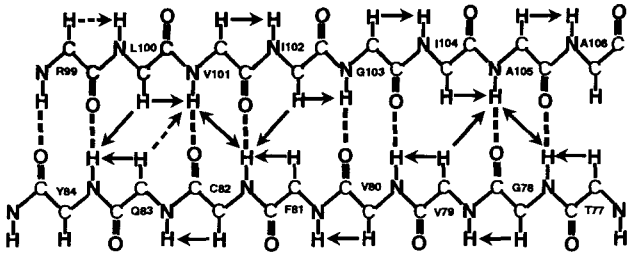

Fig. 6. The two-stranded anti-parallel β-sheet of IIA^{mtl} obtained from the analysis of the ^{15}N NOESY-HSQC and the $^{13}C\alpha$ and $^{1}H\alpha$ secondary chemical shifts. Only the ^{1}HN-^{1}HN and ^{1}HN-$^{1}H\alpha$ contacts are indicated. The solid arrows correspond to unambiguous contacts, and dashed arrows represent ambiguities due to spectral overlap.

observed amide proton resonances could be assigned. The amide ^{1}H resonances of A19, V63, and R89 were observed only at 20 °C, where exchange with water is slower. The amide ^{1}H resonances of N108–H111 and of the six N-terminal residues are not observed in the triple-resonance experiments involving the amide protons, but additional unassigned resonances are present in the COCAH spectrum, probably belonging to these missing residues.

A number of weak peaks, observed only in the HSQC spectrum (Fig. 1A), remain unassigned. All these peaks are found in the area between $\omega^{1}H$ 7.5–8.0 ppm and $\omega^{15}N$ 125–131 ppm. They show strongly negative heteronuclear ^{1}H-^{15}N NOEs (data not shown) and probably belong to the first six residues of the flexible N-terminal end.

Three of the missing backbone amide proton frequencies belong to asparagines. On the other hand, all expected side-chain resonances of the glutamine and asparagine residues are present in the HSQC spectrum of Figure 1A.

The sensitivity of the COCAH experiment is good despite the fact that the magnetogyric ratio of the ^{13}C nucleus is four times lower than that of the ^{1}H nucleus. Compared with pulse schemes that start with ^{1}H excitation, the COCAH approach has the advantage that it uses fewer rf pulses and that the Hα resonances coinciding with the residual water resonance are not attenuated by presaturation of the water signal. A disadvantage is that a longer relaxation delay is necessary due to the longer T_1's of the ^{13}CO spins.

Lengeler (1990) divided the EIIs of the PTS into different families using sequence comparisons. IIA^{glc} belongs to the glucopyranoside family and IIA^{mtl} of *E. coli* belongs to the D-mannitol/D-fructose family. The structures of IIA^{glc} from *E. coli* and *B. subtilis* have been determined using NMR and X-ray (Liao et al., 1991; Pelton et al., 1991; Worthylake et al., 1991; Fairbrother et al., 1992). The proteins are 41% homologous in their amino acid sequence and are phosphorylated at a histidine through interaction with P-HPr. The consensus sequence surrounding the phosphorylation site, present in all proteins of the glucopyranoside PTS family, is XXHXGX, were X is a hydrophobic residue (Fig. 7). The secondary structures of IIA^{glc} from *B. subtilis* and *E. coli* contain a large amount of β-sheet and some small regions with helical structure. Domain IIA^{mtl} of *E. coli*, however, contains five regions with helical structure and only two β-strands forming an anti-parallel β-sheet (Fig. 6).

IIA^{mtl} of *E. coli* from the D-mannitol/D-fructose family has a 41% sequence homology with IIA^{mtl} of *Enterococcus faecalis* and 38% homology with IIA^{mtl} of *Staphylococcus carnosus* (Fischer et al., 1991). The consensus sequence around the phosphorylation site of *E. coli* IIA^{mtl}, AXPHGT (X being a hydrophobic residue), is conserved in these three proteins (Fig. 7) and is also found in the N-terminal part of the FPr of *Salmonella typhimurium* (Geerse & Postma, 1989). The residues adjacent to the histidine in the phosphorylation site of the proteins belonging to the glucopyranoside PTS family are different from the ones found in the proteins of the D-mannitol/D-fructose PTS family. These residues are not as well conserved throughout the glucopyranoside PTS family as is the case for the D-mannitol/D-fructose PTS family. IIA^{mtl} of *E. coli* is the first protein of the D-mannitol/D-fructose PTS family for which the secondary structure has been determined.

Comparing the amino acid sequence and structural features of the IIA proteins, we postulate that there are at least two distinct classes of IIA proteins. One class of structures, the glucopyranoside PTS family (Lengeler, 1990), which includes IIA^{glc} of *E. coli* and *B. subtilis*, primarily contains a large amount of β-sheet. Another class of structures, the D-mannitol/D-fructose PTS family, which includes *E. coli* IIA^{mtl}, contains more helical elements. Considering that *E. coli* IIA proteins of both families are phosphorylated by the same P-HPr, it is reasonable to suggest that the histidine at the phosphorylation site is probably situated in a comparable environment.

The assignment of the side-chain ^{1}H and ^{13}C resonances, which is the next step toward the determination of the structure of the IIA^{mtl} domain, is in progress.

Materials and methods

Bacterial strains and growth

^{15}N-enriched protein was obtained by growing *E. coli* strain JM101 (Δ(Lac-ProAB), thi, [F′, traD36, ProAB, $LacI^{q}$, ZΔM15]) containing the plasmid pMcCI (Van Weeghel et al., 1991) at 37 °C on mineral medium containing 5 g/L D-glucose, 1 g/L $(^{15}NH_4)_2SO_4$ (95% ^{15}N enriched; VEB Berlin Chemie), 20 mg/L chloramphenicol, 1 mg/L thiamine, 0.77 μM $MgSO_4$, and 0.077 μM $CaCl_2$.

$^{15}N/^{13}C$-enriched protein was obtained by growing *E. coli* JM101 containing the plasmid pMcCI at 37 °C on mineral medium containing 1 g/L $[^{13}C_6]$-D-glucose (90% ^{13}C enriched; Cambridge Isotope Laboratories), 1 g/L $(^{15}NH_4)_2SO_4$ (99.9% ^{15}N enriched; ISOTEC Inc.),

A

```
IIA^glc (E. co)   1  M G L F D K L K S L V S D D K K D T G T I E I I A P L S G E I V N I E
IIA^glc (B. su)   1  - - - - - - - - M I A E P L Q N E I G E E V F V S P I T G E I H P I T

IIA^glc (E. co)  36  D V P D V V F A E K I V G D G I A I K P T G N K M V A P V D G T I G K
IIA^glc (B. su)  28  D V P D Q V F S G K M M G D G F A I L P S E G I V V S P V R G K I L N

IIA^glc (E. co)  71  I F E T N H A F S I E S D S G V E L F V H F G I D T V E L K G E G F K
IIA^glc (B. su)  63  V F P T K H A I G L Q S D G G R E I L I H F G I D T V S L K G E G F T

IIA^glc (E. co) 106  R I A E E G Q R V K V G D T V I E F D L P L L E E K A K S T L T P V V
IIA^glc (B. su)  98  S F V S E G D R V E P G Q K L L E V D L D A V K P N V P S L M T P I V

IIA^glc (E. co) 141  I S N M D E I K E L - I K L S G S V T V G E T P V I R I K K
IIA^glc (B. su) 133  F T N L A E G E T V S I K A S G S V N R E Q E D I V K I E K
```

B

```
IIA^mtl (E. co) 495  L F K L G A E N I F L G R K A A T K E E A I R F A G E Q L V K G G Y V
IIA^mtl (E. fa)   1  M E N L T N I S I E L N Q Q F N T K E E A I R F S G Q K L V E A G C V
IIA^mtl (S. ca)   1  T E L F S N E N I F L N Q S F E D Q N E A I E K A G Q A L V D A G A V
FPr     (S. ty)   1  M F Q L S V Q D I H P G E Q A G N K E E A I R G I A A A L A G A G N V

IIA^mtl (E. co) 526  E P E Y V Q A M L D R E K L T P T Y L G E S I A V P H G T V E A K D R
IIA^mtl (E. fa)  36  E P A Y I E A M I E R D Q L L S A H M G N F I A I P H G T E E A K K L
IIA^mtl (S. ca)  36  T E D Y I Q A M K D R E A V V S T F M G N G L A I P H G T D E A K S A
FPr     (S. ty)  36  A G G Y V D G M L A R E Q Q T S T F L G N G I A I P H G T T D T R D Q

IIA^mtl (E. co) 561  V L K T G V V F C Q Y P E G V R F G E E E D D - I A R L V I G I A A R
IIA^mtl (E. fa)  71  V K K S G I C V V Q V P E G V N F G T E E D E K I A T V L F G I A G V
IIA^mtl (S. ca)  71  V L Q S G L T L L Q I P E G V Q W G - - - D D - V A K V V V G I A G K
FPr     (S. ty)  71  V L K T G V Q V F Q F P Q G V T W G E - - G Q - V A Y V A I G I A A S

IIA^mtl (E. co) 595  N N E H I Q V I T S L T N A L D D E S V I E R L A H T T S V D E V L E
IIA^mtl (E. fa) 106  G E E H L Q L V Q Q I A L Y C S D M D N V V Q L A D A L S K E E I T E
IIA^mtl (S. ca) 102  D G E H L D L L S K I A I T F S E E E N V D R I V N T K S P E E I K A
FPr     (S. ty) 103  S D E H L G L L R Q L T H V L S D D S V A E Q L K S A T T A E E L R A

IIA^mtl (E. co) 630  L L A G R K
IIA^mtl (E. fa) 137  N L A I A
IIA^mtl (S. ca) 141  V F E E A D V
FPr     (S. ty) 138  L L M G E K Q
```

Fig. 7. Alignment of IIA proteins from (**A**) the glucopyranoside family of *E. coli* (E. co) and *B. subtilis* (B. su) (Liao et al., 1991) and (**B**) the D-mannitol/D-fructose family of *E. coli* (E. co), *E. faecalis* (E. fa), *S. carnosus* (S. ca), and *S. typhimurium* (S. ty) (Fischer et al., 1991). Conserved residues are shown in boldface type and underlined, and the phosphorylation sites are shown in italics.

20 mg/L chloramphenicol, 1 mg/L thiamine, 0.77 μM $MgSO_4$, and 0.077 μM $CaCl_2$.

Synthesis of IIA^{mtl} was induced by adding IPTG to a concentration of 1 mM to the medium immediately after inoculation. The bacteria were allowed to grow for 24 h, after which they were harvested by centrifugation (10,000 × *g*, 4 °C, 10 min).

Purification and sample preparation

IIA^{mtl} was purified as described by Van Dijk et al. (1992).

A sample of ^{15}N-enriched IIA^{mtl} in H_2O was obtained by dialyzing the purified protein solution against 2 mM KP_i, pH 7.5. After freeze drying, the protein was dissolved in 0.5 mL $H_2O/^2H_2O$ (93:7 by volume), to yield 2 mM protein solution in 50 mM KP_i, pH 7.5. The ^{15}N enrichment of the protein was more than 90%, as estimated from the intensity of the ^{15}N-coupled proton resonances in the ^1H NMR spectrum.

Samples of $^{15}N/^{13}C$-enriched IIA^{mtl} in H_2O were obtained by dialyzing the protein solution against 4 mM KP_i, pH 7.3. After freeze drying, the protein was dissolved in 1.0 mL $^1H_2O/^2H_2O$ (93:7 by volume) and divided into two aliquots, each containing a 4 mM protein solution in 50 mM KP_i, pH 7.3. The ^{13}C and ^{15}N enrichments were estimated to be approximately 80% and 90%, respectively, as described for the ^{15}N-enriched sample.

For experiments in ^2H_2O, the sample in ^1H_2O was freeze dried and redissolved in 0.5 mL ^2H_2O.

The protein concentration was determined using the Bradford method (Bradford, 1976) with bovine serum albumin as the standard.

Purity and activity

The purity of the protein was checked by denaturing SDS-PAGE on 15% gels as described by Laemmli (1970), followed by staining with Coomassie brilliant blue. The

protein migrated on gel as a single band and showed no loss of activity during the NMR experiments.

The activity of IIA^{mtl} was measured in a complementation assay described by Van Weeghel et al. (1991).

^{15}N-^{1}H heteronuclear NMR spectroscopy

All NMR experiments were performed on a Varian Unity 500-MHz spectrometer.

The 3D NOESY-HSQC and 3D TOCSY-HSQC spectra were recorded at 20 °C and 30 °C using published pulse sequences (Marion et al., 1989a,b; Fesik & Zuiderweg, 1990; Norwood et al., 1990). The spectral widths in the ω1 (^{1}H), ω2 (^{15}N), and ω3 (^{1}H) domains of the spectra recorded at 30 °C were 5,000, 2,000, and 6,667 Hz, respectively. The maximum values for t_1, t_2, and t_3 were 30, 32, and 307 ms. The spectral widths of the spectra recorded at 20 °C were 6,000, 2,000, and 7,000 Hz for ω1, ω2, and ω3, respectively. The maximum values for t_1, t_2, and t_3 were 25, 32, and 146 ms. In order to obtain quadrature detection in ω1 and ω2, TPPI was used (Bodenhausen et al., 1980).

The ^{1}H-carrier frequency was positioned at the water resonance, and the ^{15}N carrier was set at 116.6 ppm relative to liquid NH_3 (Live et al., 1984).

The mixing time in both NOESY-HSQC experiments was 100 ms, including a 20-ms homospoil pulse in the middle of this period in order to remove any coherences of order one and higher.

The spin-lock period in the TOCSY-HSQC experiments was 55 ms. A DIPSI-2 sequence (Shaka et al., 1988) was used with a $\gamma B_1 = 11$ kHz rf field.

Water was suppressed by a weak rf field during the 1-s preparation period and by two orthogonal spin-lock pulses, of 2 and 6 ms, applied during the reversed-INEPT part of the pulse sequence (Messerle et al., 1989). During acquisition, a broadband WALTZ-16 sequence (Shaka et al., 1983) with an rf field of $\gamma B_1 = 0.8$ kHz was used for ^{15}N decoupling.

^{1}H-^{15}N-^{13}C triple-resonance NMR spectroscopy

The HNCA, HN(CO)CA, and HNCO spectra were recorded using a constant-time ^{13}C-evolution period, as described by Grzesiek and Bax (1992). Both HNCA and HN(CO)CA spectra were recorded at 20 °C and 30 °C; the HNCO and COCAH spectra were recorded at 30 °C.

The ^{1}H and ^{15}N carriers were at the same positions as in the ^{15}N heteronuclear experiments. For $^{13}C\alpha$ pulses, the carrier was positioned at 58.09 ppm, and for ^{13}CO pulses, at 177.4 ppm relative to TSP (Bax & Subramanian, 1986).

The spectral widths in the ^{15}N, $^{13}C\alpha$, ^{13}CO, and ^{1}H domains were 2,000, 5,000, 2,200, and 7,000 Hz, respectively. The maximum values for t_1 (^{15}N), t_2 (^{13}C), and t_3 (^{1}H) were 20, 9.6, and 73 ms in the HNCA experiment; 16, 12.8, and 73 ms in the HN(CO)CA experiment; and 16, 21.8, and 73 ms in the HNCO experiment. The maximum values for t_1 (^{13}CO), t_2 ($^{13}C\alpha$), and t_3 (^{1}H) in the COCAH experiment were 14.5, 10.8, and 73 ms. Quadrature detection in ω1 and ω2 was done by TPPI. The water signal was suppressed by a weak rf field during the preparation period of 1 s.

The COCAH experiment is comparable to the HCACO experiment described by Powers et al. (1991). Instead of starting the experiment with a 90° ^{1}H-pulse, it starts with a 90° ^{13}CO-pulse. The pulse sequence includes two constant-time ^{13}C-evolution periods and is shown in Figure 8.

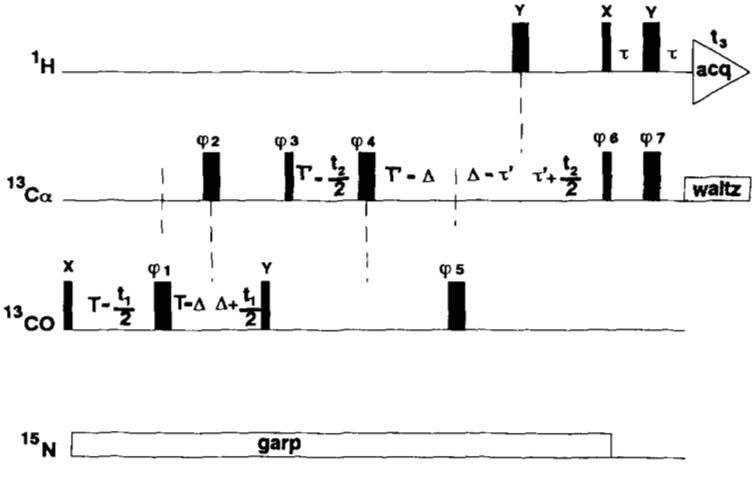

Fig. 8. Pulse sequence of the COCAH. The small pulses correspond to 90° pulses, the broad pulses to 180° pulses. The durations of the delays are $\tau = 1.7$ ms, $\tau' = 1.2$ ms, $\Delta = 4.5$ ms, $2T = 15$ ms, and $2T' = 11$ ms. Phase cycling was as follows: $\varphi_1 = 4(y, -x, -y, x)$; $\varphi_2 = 8(y), 8(-y)$; $\varphi_3 = 8(x), 8(-x)$; $\varphi_4 = 2(y, y, -x, -x, -y, -y, x, x)$; $\varphi_5 = 8(y), 8(-y)$; $\varphi_6 = 8(x), 8(-x)$; $\varphi_7 = 4(y), 4(-x), 4(-y), 4(x)$; Acq. $= 4(x, -x, -x, x)$. During the acquisition, ^{13}C decoupling was achieved by a WALTZ-16 decoupling sequence with an rf field of $\gamma B_1 = 0.8$ kHz. ^{15}N decoupling during both evolution periods was achieved by a GARP decoupling sequence (Shaka et al., 1985). A 1-s water presaturation period was included in the 1.9-s preparation period. The spectral widths in the ^{13}CO (ω_1), $^{13}C\alpha$ (ω_2), and ^{1}H (ω_3) domain were 2,200 Hz, 5,000 Hz, and 7,000.4 Hz, respectively. The maximum values for t_1, t_2, and t_3 were 10.8 ms, 14.5 ms, and 73 ms, respectively. For each t_1, t_2 pair, 16 transients were recorded. TPPI was used on the first 90° ^{13}CO pulse and on φ_3 to discriminate between positive and negative frequencies in the t_1 and t_2 domains, respectively.

Data processing

All data were processed and analyzed on a Convex C220 using the program SNARF, written by Frans van Hoesel, Groningen.

All 3D spectra were recorded as sets of 2D spectra. The time-domain data were filtered before Fourier transformation by multiplication with a shifted sine-bell function or by a Lorentz-Gauss transformation. After Fourier transformation of the three domains, a data set of 512 × 256 × 128 real points was obtained in the case of the NOESY-HSQC and TOCSY-HSQC spectra. A data set of 512 × 128 × 128 real points was obtained for the HNCA, HN(CO)CA, and HNCO spectra. The COCAH spectrum consisted of 790 × 128 × 128 real points.

Acknowledgments

This research was supported by the Netherlands Foundation for Chemical Research (SON). J. Grötzinger was supported by the BRIDGE program of the European Community (BIOT-913029).

We thank Varian for providing us with the triple-resonance probe and T. Nowak for assistance in acquiring the [$^{13}C_6$]glucose. We thank A.A. van Dijk and G.K. Wolters for their help with the isolation and purification of IIA^{mtl}, N.A.J. van Nuland for helpful advice and comments, and Frans van Hoesel for writing the program SNARF, which we used for processing, visualizing, and analyzing all NMR data sets.

References

Bax, A. & Subramanian, S. (1986). Sensitivity-enhanced two-dimensional heteronuclear shift correlation NMR spectroscopy. *J. Magn. Reson. 67*, 565–569.

Billeter, M., Braun, W., & Wüthrich, K. (1982). Sequential resonance assignments in protein ^{1}H nuclear magnetic resonance spectra. Computation of sterically allowed proton–proton distances and statistical analysis of proton–proton distances in single crystal protein conformation. *J. Mol. Biol. 155*, 321–346.

Bodenhausen, G. & Ruben, D.J. (1980). Natural abundance nitrogen-15 NMR by enhanced heteronuclear spectroscopy. *Chem. Phys. Lett. 69*, 185–189.

Bodenhausen, G., Vold, R.L., & Vold, R.R. (1980). Multiple quantum spin-echo spectroscopy. *J. Magn. Reson. 37*, 93–106.

Bradford, M.M. (1976). A rapid and sensitive method for the quantitation of microgram quantities of protein utilizing the principle of protein–dye binding. *Anal. Biochem. 72*, 248–254.

Fairbrother, W.J., Cavanagh, J., Dyson, J., Palmer, A.G., III, Sutrina, S.L., Reizer, J., Saier, M.H., Jr., & Wright, P.E. (1991). Polypeptide backbone resonance and secondary structure of *Bacillus subtilis* enzyme III^{glc} determined by two-dimensional and three-dimensional heteronuclear NMR spectroscopy. *Biochemistry 30*, 6896–6907.

Fairbrother, W.J., Gippert, G.P., Reizer, J., Saier, M.H., Jr., & Wright, P.E. (1992). Low resolution structure of the *Bacillus subtilis* glucose permease IIA domain derived from heteronuclear three-dimensional NMR spectroscopy. *FEBS Lett. 296*, 148–152.

Fesik, S.W. & Zuiderweg, E.R.P. (1990). Heteronuclear three-dimensional NMR spectroscopy of isotopically labelled biological macromolecules. *Q. Rev. Biophys. 23*, 97–131.

Fischer, R., von Strandmann, R.P., & Hengstenberg, W. (1991). Mannitol-specific phosphoenolpyruvate-dependent phospho-transferase system of *Enterococcus faecalis*: Molecular cloning and nucleotide sequences of the enzyme III^{mtl} gene and the mannitol-1-phosphate dehydrogenase gene, expression in *Escherichia coli*, and comparison of the gene products with similar enzymes. *J. Bacteriol. 173*, 3709–3715.

Geerse, R.H. & Postma, P.W. (1989). The PEP fructose phosphotransferase system in *Salmonella typhimurium*. FPr combines enzyme III^{fru} and pseudo-HPr activities. *Mol. Gen. Genet. 216*, 517–525.

Grzesiek, S. & Bax, A. (1992). Improved 3D triple-resonance NMR techniques applied to a 31 kDa protein. *J. Magn. Reson. 96*, 432–440.

Haris, P.I., Robillard, G.T., Van Dijk, A.A., & Chapman, D. (1992). Potential of ^{13}C and ^{15}N labeling for studying protein–protein interactions using Fourier transform infrared spectroscopy. *Biochemistry 31*, 6279–6284.

Howarth, O.W. & Lilley, D.M.J. (1978). Carbon-13-NMR of peptides and proteins. *Progr. NMR Spectrosc. 12*, 1–40.

Laemmli, U.K. (1970). Cleavage of structural proteins during the assembly of the head of bacteriophage T4. *Nature 227*, 680–685.

Lengeler, J.W. (1990). Molecular analysis of the enzyme II-complexes of the bacterial phosphotransferase system (PTS) as carbohydrate transport systems. *Biochim. Biophys. Acta 108*, 155–159.

Liao, D.-I., Kapadia, G., Reddy, P., Saier, M.H., Jr., Reizer, J., & Herzberg, O. (1991). Structure of the IIA domain of the glucose permease of *Bacillus subtilis* at 2.2-Å resolution. *Biochemistry 30*, 9583–9594.

Live, D.H., Davis, D.G., Agosta, W.C., & Cowburn, D. (1984). Long range hydrogen bond mediated effects in peptides: ^{15}N NMR study of gramicidin S in water and organic solvents. *J. Am. Chem. Soc. 106*, 1939–1941.

Lolkema, J.S. & Robillard, G.T. (1992). The enzymes II of the phosphoenolpyruvate-dependent carbohydrate transport systems. In *The New Comprehensive Biochemistry: Pumps, Carriers and Channels* (de Pont, J.J.H.M.M., Ed.), pp. 135–167. Elsevier/North Holland Biomedical Press, Amsterdam.

Marion, D., Driscoll, P.C., Kay, L.E., Wingfield, P.T., Bax, A., Gronenborn, A.M., & Clore, G.M. (1989a). Overcoming the overlap problem in the assignment of ^{1}H-NMR spectra of larger proteins by use of three-dimensional heteronuclear ^{1}H-^{15}N Hartmann–Hahn multiple quantum coherence and nuclear-Overhauser multiple quantum coherence spectroscopy: Application to interleukin 1β. *Biochemistry 28*, 6150–6156.

Marion, D., Kay, L.E., Sparks, S.W., Torchia, D.A., & Bax, A. (1989b). Three-dimensional heteronuclear NMR of nitrogen-15 labeled proteins. *J. Am. Chem. Soc. 111*, 1515–1517.

Meadow, N.D., Fox, D.K. & Roseman, S. (1990). The bacterial phosphoenolpyruvate:glucose phosphotransferase system. *Annu. Rev. Biochem. 59*, 497–542.

Messerle, B.A., Wider, G., Otting, G., Weber, C., & Wüthrich, K. (1989). Solvent suppression using a spin lock in 2D and 3D NMR spectroscopy with H_2O solutions. *J. Magn. Reson. 85*, 608–613.

Norwood, T.J., Boyd, J., Heritage, J.E., Soffer, N., & Campbell, I.D. (1990). Comparison of techniques for ^{1}H-detected heteronuclear ^{1}H-^{15}N spectroscopy. *J. Magn. Reson. 87*, 488–501.

Pas, H.H., Meyer, G., Kruizinga, W.H., Tamminga, K.S., Van Weeghel, R.P., & Robillard, G.T. (1991). ^{31}P phospho-NMR demonstration of phosphocysteine as a catalytic intermediate on the *Escherichia coli* phosphotransferase system EII^{mtl}. *J. Biol. Chem. 266*, 6690–6692.

Pas, H.H. & Robillard, G.T. (1988). *S*-phosphocysteine and phosphohistidine are intermediates in the phosphoenol-pyruvate dependent mannitol transport catalyzed by *Escherichia coli* EII^{mtl}. *Biochemistry 27*, 5835–5839.

Pas, H.H., Ten Hoeve-Duurkens, R.H., & Robillard, G.T. (1988). Bacterial phosphoenolpyruvate dependent phosphotransferase system: Mannitol-specific EII contains two phosphoryl binding sites per monomer and one high-affinity mannitol binding site per dimer. *Biochemistry 27*, 5520–5525.

Pelton, J.G., Torchia, D.A., Meadow, N.D., Wong, C.Y., & Roseman, S. (1991). Secondary structure of the phosphocarrier protein III^{glc}, a signal-transducing protein from *Escherichia coli*, determined by heteronuclear three-dimensional NMR spectroscopy. *Proc. Natl. Acad. Sci. USA 88*, 3479–3483.

Postma, P.W. & Lengeler, J.W. (1985). Phosphoenolpyruvate:carbohydrate phosphotransferase system of bacteria. *Microbiol. Rev. 49*, 232–269.

Powers, R., Gronenborn, A.M., Clore, M.C., & Bax, A. (1991). Three-dimensional triple-resonance NMR of $^{13}C/^{15}N$-enriched proteins using constant-time evolution. *J. Magn. Reson. 94*, 209–213.

Shaka, A.J., Barker, P.B., & Freeman, R. (1985). Computer-optimized decoupling scheme for wideband applications and low-level operation. *J. Magn. Reson. 64*, 547–552.

Shaka, A.J., Keeler, J., & Freeman, R. (1983). Evaluation of a new broadband decoupling sequence: WALTZ-16. *J. Magn. Reson. 53*, 313–340.

Shaka, A.J., Lee, C.J., & Pines, A. (1988). Iterative schemes for bilinear operators; application to spin decoupling. *J. Magn. Reson. 77*, 274–293.

Spera, S. & Bax, A. (1991). Empirical correlation between protein backbone conformation and Cα and Cβ ^{13}C nuclear magnetic resonance chemical shifts. *J. Am. Chem. Soc. 113*, 5490–5492.

Van Dijk, A.A. (1992). Phosphorylation in the mannitol specific PTS. Aspects of the phosphoenol-pyruvate dependent phosphotransferase system (PTS) in *Escherichia coli*, pp. 53–67. Thesis, State University of Groningen, Groningen, The Netherlands.

Van Dijk, A.A., Scheek, R.M., Dijkstra, K., Wolters, G.K., & Robillard, G.T. (1992). Characterization of the protonation and hydrogen bonding state of the histidine residues in IIA^{mtl}, a domain of the phosphoenolpyruvate-dependent mannitol-specific transport protein. *Biochemistry 31*, 9063–9072.

Van Nuland, N.A.J., Kroon, G.J.A., Dijkstra, K., Wolters, G.K., Scheek, R.M., & Robillard, G.T. (1993). The determination of the IIA^{mtl} binding site on HPr of the *Escherichia coli* phosphoenolpyruvate-dependent phospho-transferase system. *FEBS Lett. 315*, 11–15.

Van Nuland, N.A.J., Van Dijk, A.A., Dijkstra, K., Van Hoesel, F.H.J., Scheek, R.M., & Robillard, G.T. (1992). Three-dimensional ^{15}N-^{1}H-^{1}H and ^{15}N-^{13}C-^{1}H nuclear-magnetic resonance studies of HPr, a central component of the phosphoenolpyruvate-dependent phosphotransferase system from *Escherichia coli*. *Eur. J. Biochem. 203*, 483–491.

Van Weeghel, R.P., Meyer, G., Keck, W.H., & Robillard, G.T. (1991). Phosphoenolpyruvate-dependent mannitol phospho-transferase system of *Escherichia coli*: Overexpression, purification, and characterization of the enzymatically active C-terminal domain of enzyme II^{mtl} equivalent to enzyme III^{mtl}. *Biochemistry 30*, 1774–1779.

Wishart, D.S., Sykes, B.D., & Richards, F.M. (1992). The chemical shift index: A fast and simple method for the assignment of protein secondary structure through NMR spectroscopy. *Biochemistry 31*, 1647–1651.

Worthylake, D., Meadow, N.D., Roseman, S., Liao, D.-I., Herzberg, O., & Remmington, S.J. (1991). Three-dimensional structure of the *Escherichia coli* phosphocarrier protein III^{glc}. *Proc. Natl. Acad. Sci. USA 88*, 20382–20386.

Wüthrich, K. (1986). *NMR of Proteins and Nucleic Acids*, pp. 117–176. Wiley, New York.